Supplementary Information (SI) for Journal of Materials Chemistry C.
This journal is © The Royal Society of Chemistry 2025

Electronic Supplementary Information

Insights into the Thermal Decomposition and Conversion Mechanism of Nickel Xanthates to Nickel Sulfides

Melissa Sophie Egger[a], Marco Sigl[a], Robert Saf[a], Heinz Amenitsch[b], Ana Torvisco[b], Thomas Rath[a]*, Gregor Trimmel[a]*

[a] Institute for Chemistry and Technology of Materials (ICTM), NAWI Graz, Graz University of Technology, Stremayrgasse 9, 8010 Graz, Austria

[b] Institute of Inorganic Chemistry, NAWI Graz, Graz University of Technology, Stremayrgasse 9, 8010 Graz, Austria

* Corresponding authors email addresses: T.R: thomas.rath@tugraz.at; G.T: gregor.trimmel@tugraz.at

NMR spectra

NiXaC1

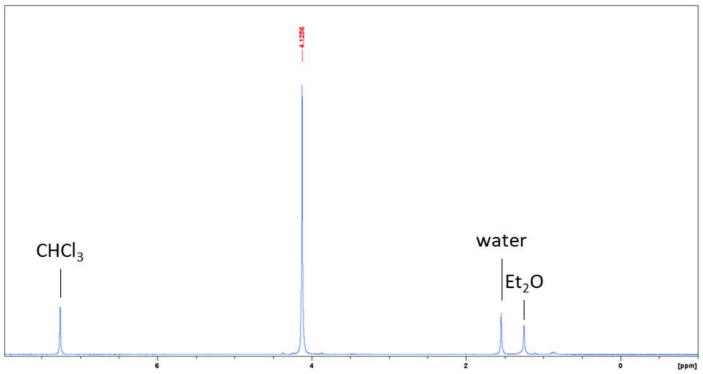

Fig. S1 1H-NMR spectrum (300 MHz, D2O) of Nickel (II)-O-methyl-dithiocarbonate (NiXaC1): δ = 4.13 (s, 3H, OCH3) ppm. No 13C-NMR spectrum as solubility was too low.

NiXaC2

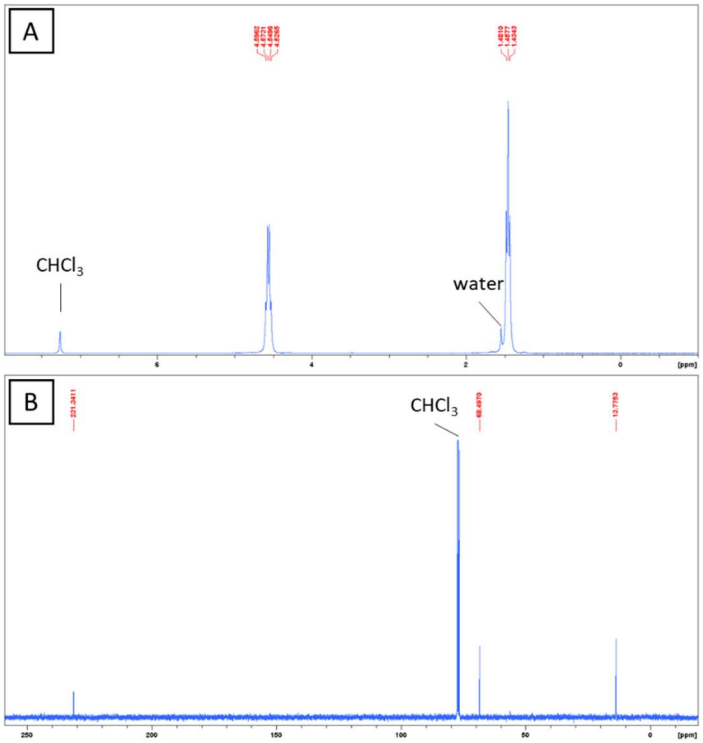

Fig. S2 A: 1H-NMR spectrum (300 MHz, D2O) of Nickel (II)-O-ethyl-dithiocarbonate (NiXaC2): δ = 4.53-4.60 (q, 2H, CH2), 1.43-1.48 (t, 3H, CH3) ppm. B: 13C-NMR spectrum (75 MHz, D2O): δ = 231.3 (CS2O), 68.5 (OCH2), 13.8 (CH3) ppm.

NiXaC3

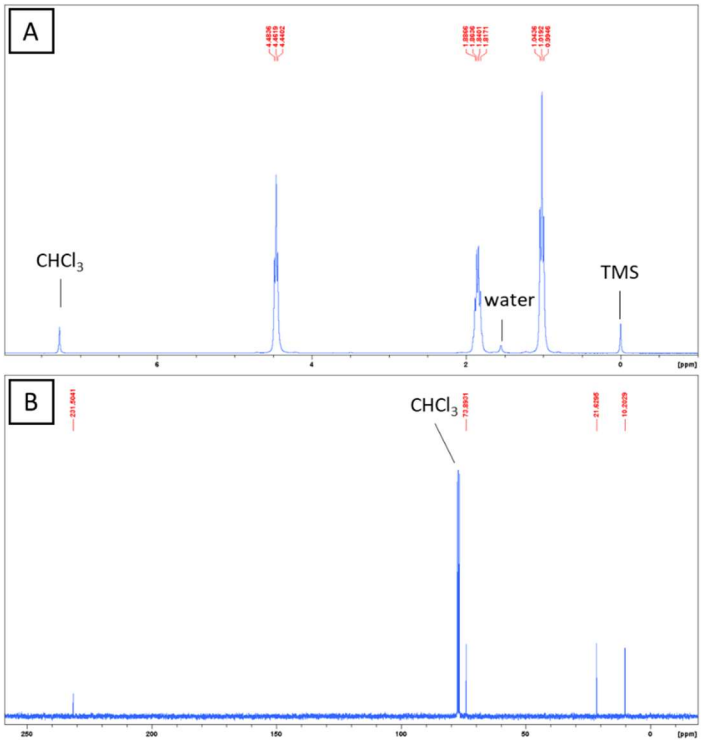

Fig. S3 A: ^{1}H NMR spectrum (300 MHz, D2O) of Nickel (II)-O-propyl-dithiocarbonate (NiXaC3): δ = 4.44-4.48 (t, 2H, CH_2), 1.82-1.89 (m, 2H, CH_2), 0.99-1.04 (t, 3H, CH_3) ppm. B: ^{13}C-NMR spectrum (75 MHz, D_2O): δ = 231.5 (CS_2O), 73.9 (OCH_2), 21.6 (CH_2), 10.2 (CH_3) ppm.

NiXaC3b

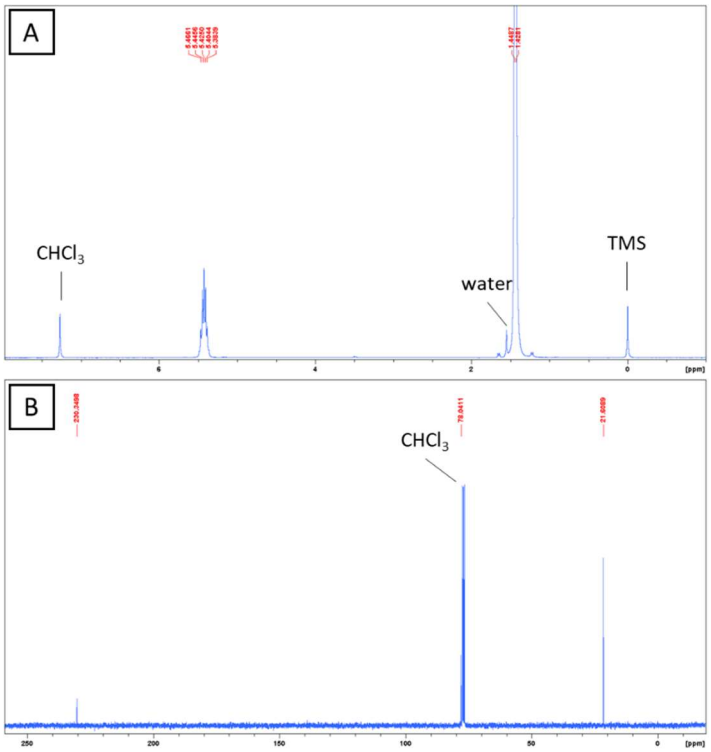

Fig. S4 A: ^{1}H NMR spectrum (300 MHz, D2O) of Nickel (II)-O-isopropyl-dithiocarbonate (NiXaC3b): δ = 5.38-5.47 (m, 1H, CH), 1.43-1.45 (d, 6H, 2xCH_3) ppm. B: ^{13}C-NMR spectrum (75 MHz, D_2O): δ = 230.3 (CS_2O), 78.1 (OCH), 21.6 (CH_3) ppm.

NiXaC4b

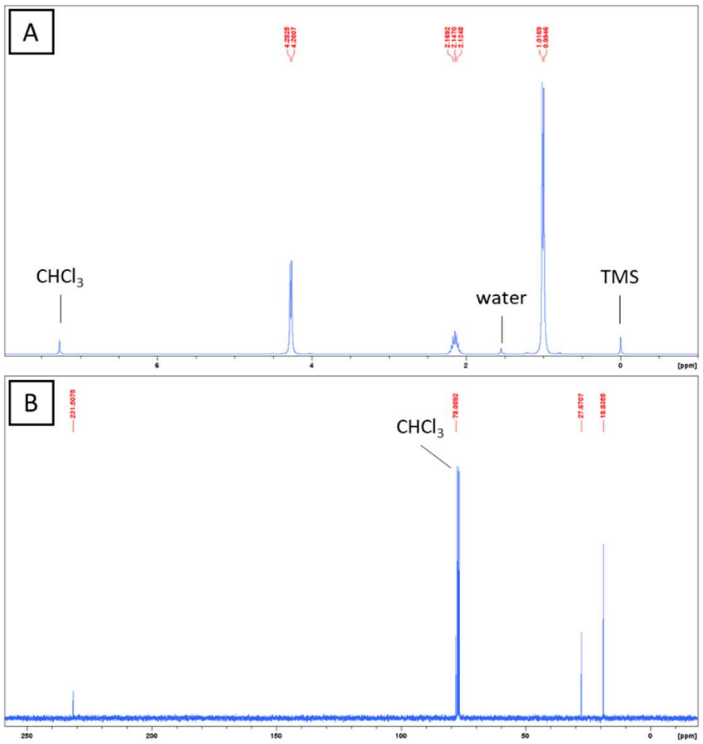

Fig. S5 A: ^{1}H NMR spectrum (300 MHz, D2O) of Nickel (II)-O-isobutyl-dithiocarbonate (NiXaC4b): δ = 4.26-4.28 (d, 2H, CH_2), 2.08-2.22 (m, 1H, CH), 0.99-1.02 (d, 6H, 2xCH_3) ppm. B: ^{13}C-NMR spectrum (75 MHz, D_2O): δ = 231.5 (CS_2O), 78.1 (OCH_2), 27.7 (CH), 18.8 (CH_3) ppm.

NiXaC5

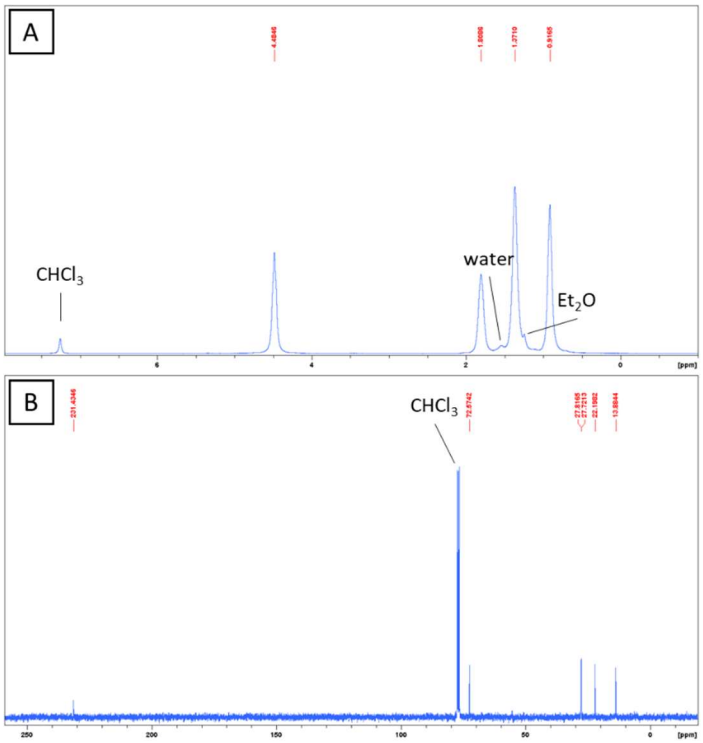

Fig. S6 A: ^{1}H NMR spectrum (300 MHz, D2O) of Nickel (II)-O-pentyl-dithiocarbonate (NiXaC5, 1f): δ = 4.47-4.51 (s, 2H, CH_2), 1.79-1,81 (s, 2H, CH_2), 1.37-1.38 (s, 4H, CH_2), 0.90-0.95 (s, 2H, CH_3) ppm, B: ^{13}C-NMR spectrum (75 MHz, D_2O): δ = 231.4 (CS_2O) 72.6 (OCH_2), 27.8 (CH_2), 27.7 (CH_2), 22.2 (CH_2), 13.9 (CH_3) ppm.

NiXaC5b

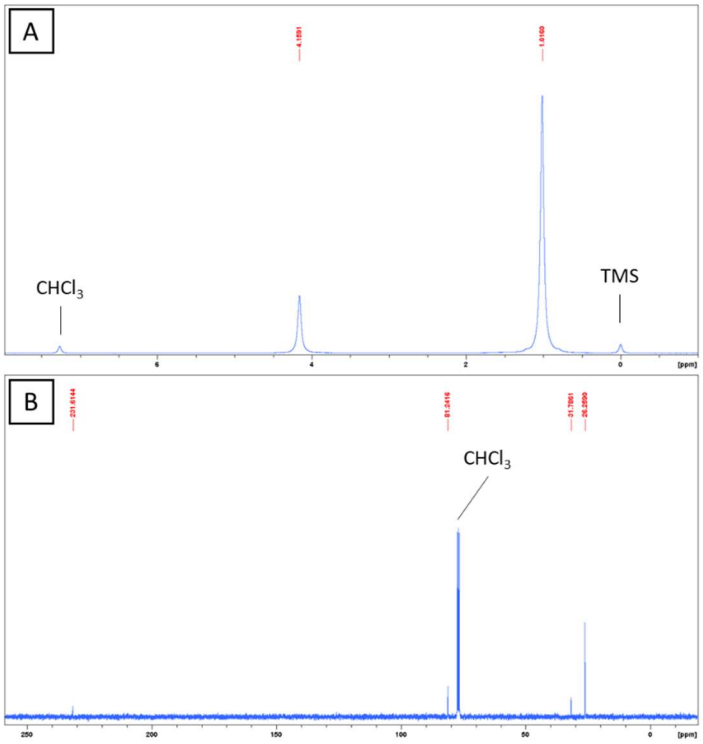

Fig. S7 A: ^{1}H NMR spectrum (300 MHz, D2O) of Nickel (II)-O-neopentyl-dithiocarbonate (NiXaC5b): δ = 4.16 (s, 2H, CH_2), 1.02 (s, 9H, 3xCH_3) ppm, B: ^{13}C-NMR spectrum (75 MHz, D_2O): δ = 231.6 (CS_2O), 81.2 (OCH_2), 31.8 (C), 26.3 (CH_3) ppm.

NiXaC6

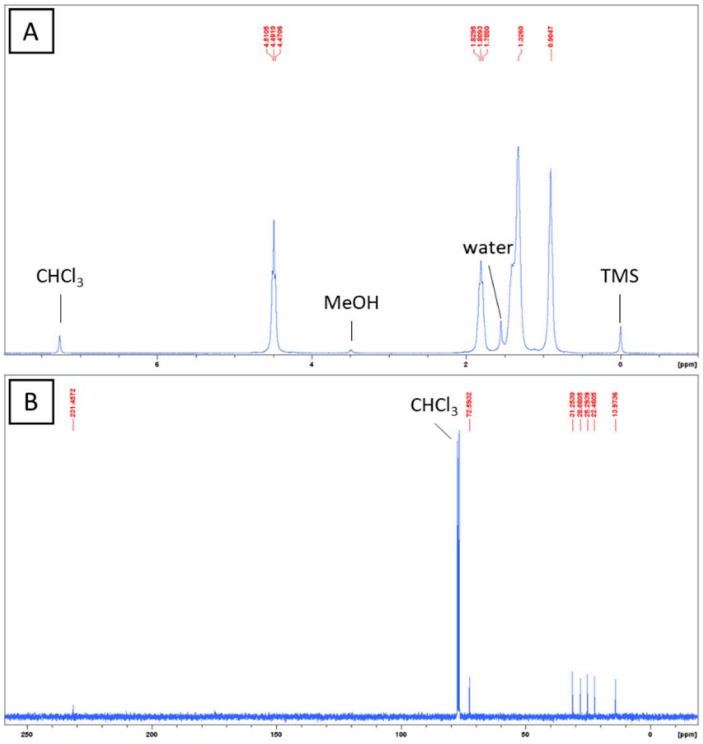

Fig. S8 A: ^{1}H NMR spectrum (300 MHz, D2O) of Nickel (II)-O-hexyl-dithiocarbonate (NiXaC6): δ = 4.47-5.51 (t, 2H, CH_2), 1.79-1.83 (m, 2H, CH_2), 1.38-1.43 (m, 4H, CH_2), 1.31-1.34 (s, 2H, CH_2), 0.88-0.93 (s, 3H, CH_3) ppm. B: ^{13}C-NMR spectrum (75 MHz, D_2O): δ = 231.5 (CS_2O), 72.6 (OCH_2), 31.3 (CH_2), 28.1 (CH_2), 25.3 (CH_2), 22.5 (CH_2), 14.0 (CH_3) ppm.

Thermogravimetric analysis

Table S1 Results of the TGA measurements for the linear and branched nickel xanthates, the corresponding TGA traces are given in Fig. 2. T_{onset} was determined as using the tangent method

Xanthate	Δm_{exp} [%]	Δm_{th} [%]	Deviation [%]	T_{onset} [°C]	T_{end} [°C]	T_m [°C]
NiXaC1	64.5	66.8	- 2.3	164	191	
NiXaC2	71.2	69.9	+ 1.4	175	221	138
NiXaC3	72.8	72.4	+ 0.4	181	222	103
NiXaC3*b*	74.5	72.4	+ 2.1	162	202	113
NiXaC4*b*	76.3	74.6	+ 1.6	213	251	140
NiXaC5	76.2	76.4	- 0.2	194	218	62
NiXaC5*b*	79.0	76.4	+ 2.5	212	242	210
NiXaC6	77.7	78.0	-0.4	198	222	61
NiXaC6*b*	76.4	78.0	- 1.6	187	212	197
NiXaC7*b*	78.5	79.4	- 1.0	177	206	161

Pyrolysis-GC-HRMS

Table S2 Pyrolysis-GC-HRMS Data for the precursor NiXaC1 (Ni-S-CS-OR)$_2$, R = Methyl). Retention times and percentages of the decomposition products with names, masses (found and calculated) and mass error

RT [min]	Area [%]	Name	Formula	Adduct/Loss	m/z calc.	m/z found	Mass error [ppm]
1.48	14.81	Carbonyl sulfide	C O S	none	59.96644	59.96647	0.50
1.50	0.12	Methanol	C H4 O	none	32.02567	32.02573	1.87
1.64	0.01	Methane thiol	C H4 S	none	48.00282	48.00272	-2.08
1.78	1.70	Dimethyl sulfide	C2 H6 S	none	62.01847	62.01852	0.81
1.87	1.78	Carbon disulfide	C S2	none	75.94359	75.94367	1.05
3.98	1.23	Dimethyl disulfide	C2 H6 S2	none	93.99054	93.99050	-0.43
4.44	1.98	O,O-Dimethyl thiocarbonate	C3 H6 O2 S	none	106.00830	106.00822	-0.75
6.97	78.05	O,S-Dimethyl dithiocarbonate	C3 H6 O S2	none	121.98546	121.98541	-0.41
7.02	0.04	S,S-Dimethyl dithiocarbonate	C3 H6 O S2	none	121.98546	121.98543	-0.25
8.38	0.26	O,O-Dimethyl dithiooxalate	C4 H6 O2 S2	none	149.98037	149.98035	-0.13
9.08	0.02	Dimethyl trithiocarbonate	C3 H6 S3	none	137.96261	137.96268	0.51

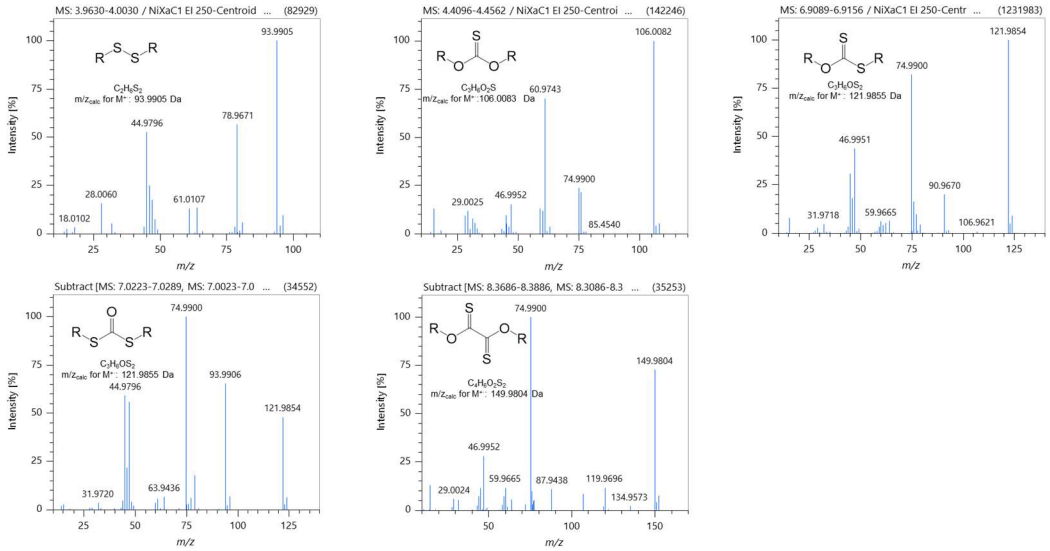

Fig. S9 Mass spectra of the decomposition products of NiXaC1. First row: dimethyl disulfide, O,O-dimethyl thiocarbonate, O,S-dimethyl dithiocarbonate. Second row: S,S-dimethyl dithiocarbonate, O,O-dimethyl dithiooxalate.

Table S3 Pyrolysis-GC MS Data for the precursor NiXaC2, $(Ni\text{-}S\text{-}CS\text{-}OR)_2$, R = Ethyl). Retention times and percentages of the decomposition products with names, masses (found and calculated) and mass error

RT [min]	Area [%]	Name	Formula	Adduct/Loss	m/z calc.	m/z found	Mass error [ppm]
1.51	11.35	Carbonyl sulfide	C O S	none	59.96644	59.96649	0.83
1.63	0.49	Ethanol	C2 H6 O	none	46.04132	46.04128	-0.87
1.73	0.03	Ethane thiol	C2 H6 S	none	62.01847	62.01855	1.29
1.88	1.81	Carbon disulfide	C S2	none	75.94359	75.94365	0.79
3.33	0.86	Diethyl sulfide	C4 H10 S	none	90.04977	90.04970	-0.78
6.46	2.44	Diethyl disulfide	C4 H10 S2	none	122.02184	122.02177	-0.57
6.54	0.46	O,S-Diethyl thiocarbonate	C5 H10 O2 S	none	134.03960	134.03957	-0.22
6.64	2.52	O,O-Diethyl thiocarbonate	C5 H10 O2 S	none	134.03960	134.03951	-0.67
8.46	79.86	O,S-Diethyl dithiocarbonate	C5 H10 O S2	none	150.01676	150.01682	0.40
9.43	0.18	O,O-Diethyl dithiooxalate	C6 H10 O2 S2	none	178.01167	178.01182	0.84

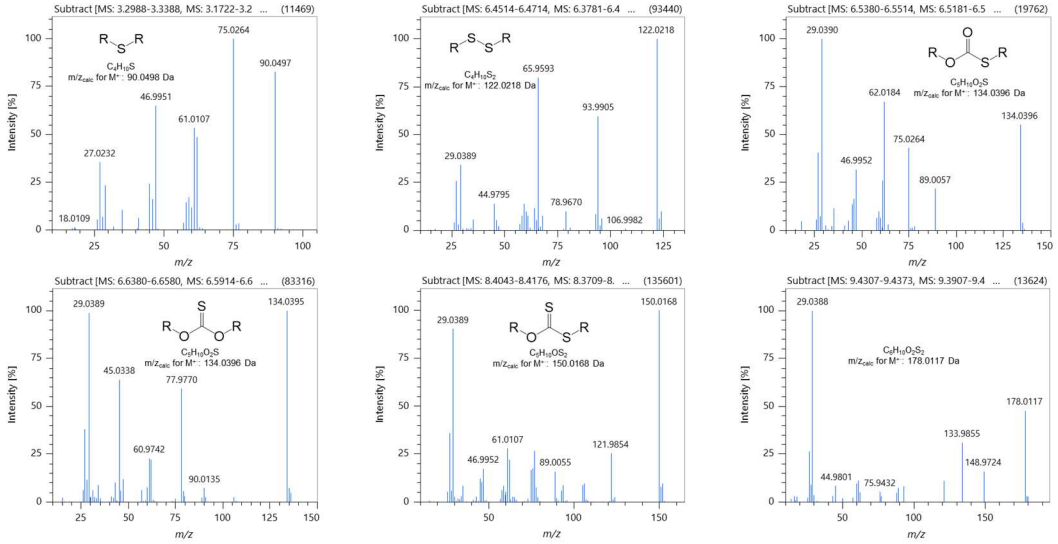

Fig. S10 Mass spectra of the decomposition products of NiXaC2. First row: diethyl sulfide, diethyl disulfide, O,S-diethyl thiocarbonate. Second row: O,O-diethyl thiocarbonate, O,S-diethyl dithiocarbonate, O,O-diethyl dithiooxalate.

Table S4 Pyrolysis-GC MS Data for the precursor NiXaC3, $(Ni\text{-}S\text{-}CS\text{-}OR)_2$, R = Propyl). Retention times and percentages of the decomposition products with names, masses (found and calculated) and mass error

RT [min]	Area [%]	Name	Formula	Adduct/Loss	m/z calc.	m/z found	Mass error [ppm]
1.49	0.06	Propene	C3 H6	none	42.04640	42.04652	2.85
1.52	7.38	Carbonyl sulfide	C O S	none	59.96644	59.96652	1.33
1.89	1.46	Carbon disulfide	C S2	none	75.94359	75.94369	1.32
1.92	0.30	1-Propanol	C3 H8 O	none	60.05697	60.05681	-2.66
2.24	0.03	1-Propane thiol	C3 H8 S	none	76.03412	76.03419	0.92
6.08	0.75	Dipropyl sulfide	C6 H14 S	none	118.08107	118.08103	-0.34
8.33	2.00	Dipropyl disulfide	C6 H14 S2	none	150.05314	150.05314	0.00
8.42	4.13	O,O-Dipropyl thiocarbonate	C7 H14 O2 S	none	162.07090	162.07097	0.43
9.93	83.54	O,S-Dipropyl dithiocarbonate	C7 H14 O S2	none	178.04806	178.04838	1.80
10.66	0.35	O,O-Dipropyl dithiooxalate	C8 H14 O2 S2	none	206.04297	206.04306	0.44

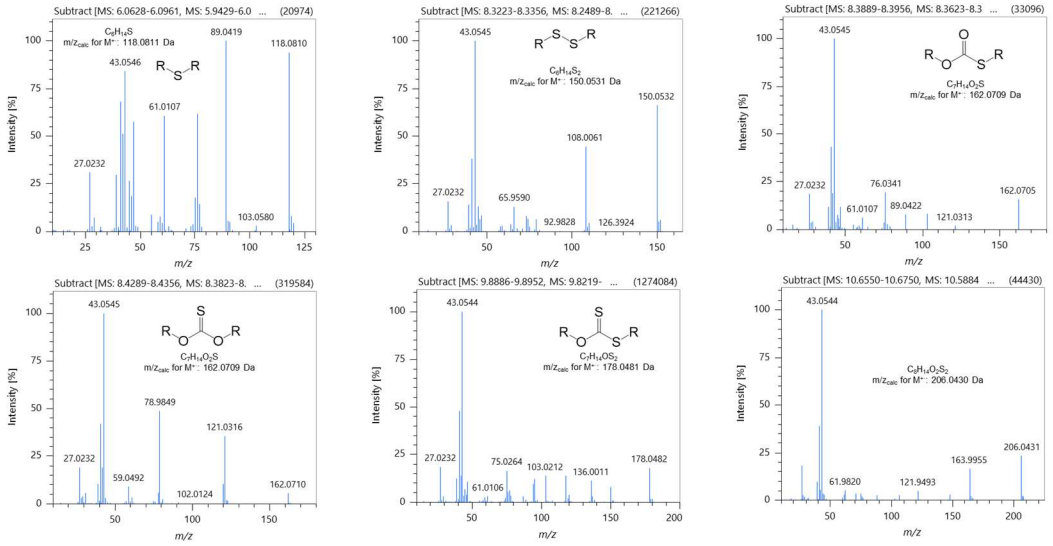

Fig. S11 Mass spectra of the decomposition products of NiXaC3. First row: dipropyl sulfide, dipropyl disulfide, O,S-dipropyl thiocarbonate. Second row: O,O-dipropyl thiocarbonate, O,S-dipropyl dithiocarbonate, O,O-dipropyl dithiooxalate.

Table S5 Pyrolysis-GC MS Data for the precursor NiXaC3b, $(Ni\text{-}S\text{-}CS\text{-}OR)_2$, R = iso-Propyl). Retention times and percentages of the decomposition products with names, masses (found and calculated) and mass error

RT [min]	Area [%]	Name	Formula	Adduct/Loss	m/z calc.	m/z found	Mass error [ppm]
1.49	39.36	Carbonyl sulfide	C O S	none	59.96644	59.96643	-0.17
1.71	0.44	Isopropanol	C3 H8 O	-CH3	45.03349	45.03368	4.22
1.87	0.35	Carbon disulfide	C S2	none	75.94359	75.94360	0.13
1.95	17.76	Isopropane thiol	C3 H8 S	none	76.03412	76.03414	0.26
4.73	12.57	Diisopropyl sulfide	C6 H14 S	none	118.08107	118.08091	-1.36
7.42	0.22	O,O-Diisopropyl thiocarbonate	C7 H14 O2 S	none	162.07090	162.07039	-3.15
7.52	21.28	Diisopropyl disulfide	C6 H14 S2	none	150.05314	150.05294	-1.33
9.00	0.89	O,S-Diisopropyl dithiocarbonate	C7 H14 O S2	none	178.04806	178.04787	-1.07
9.04	7.05	S,S-Diisopropyl dithiocarbonate	C7 H14 O S2	none	178.04806	178.04795	-0.62
9.36	0.06	Diisopropyl trisulfide	C6 H14 S3	none	182.02521	182.02486	-1.92

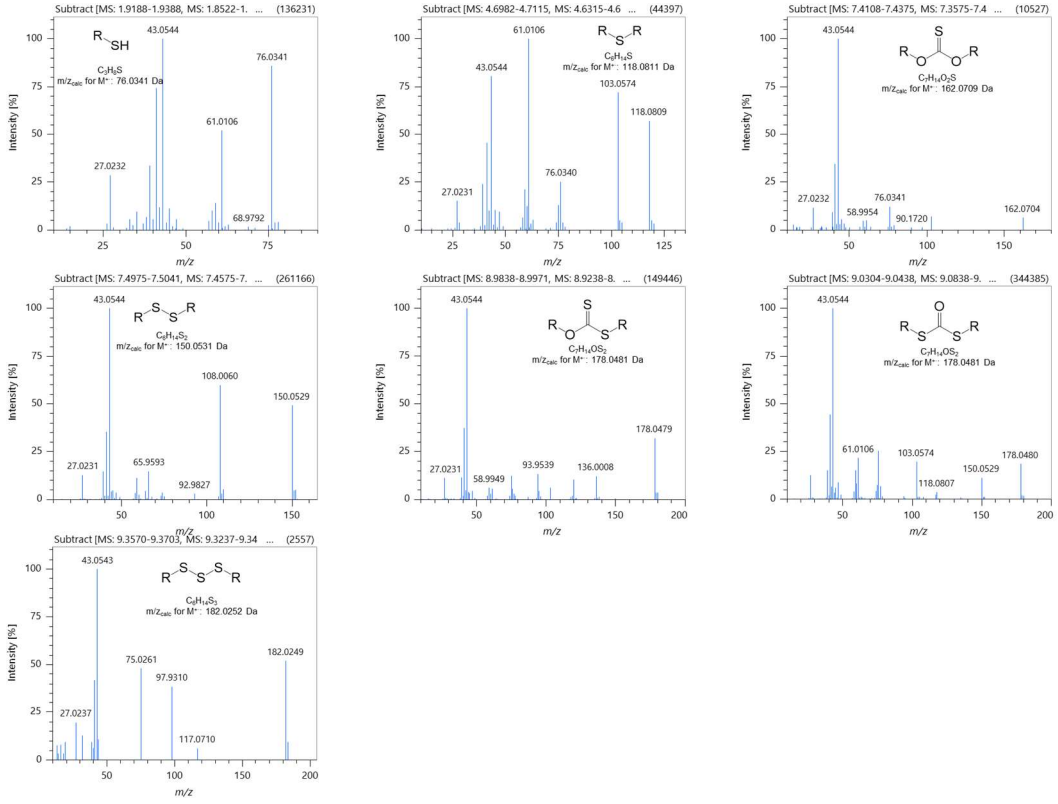

Fig. S12 Mass spectra of the decomposition products of NiXaC3b. First row: isopropane thiol, diisopropyl sulfide, O,O-diisopropyl thiocarbonate. Second row: diisopropyl disulfide, O,S-diisopropyl dithiocarbonate, S,S-diisopropyl dithiocarbonate. Third row: Diisopropyl trisulfide.

Table S6 Pyrolysis-GC MS Data for the precursor NiXaC4b, $(Ni\text{-}S\text{-}CS\text{-}OR)_2$, R = iso-Butyl). Retention times and percentages of the decomposition products with names, masses (found and calculated) and mass error

RT [min]	Area [%]	Name	Formula	Adduct/Loss	m/z calc.	m/z found	Mass error [ppm]
1.51	0.36	2-Methylpropene	C4 H8	none	56.06205	56.06216	1.96
1.61	2.45	Carbonyl sulfide	C O S	none	59.96644	59.96652	1.33
1.95	2.66	Carbon disulfide	C S2	none	75.94359	75.94370	1.45
2.37	0.04	Isobutanol	C4 H10 O	none	74.07262	74.0725	-1.62
3.23	0.03	Isobutane thiol	C4 H10 S	none	90.04977	90.04984	0.78
7.28	0.13	Diisobutyl sulfide	C8 H18 S	none	146.11237	146.11253	1.10
9.16	0.34	Diisobutyl disulfide	C8 H18 S2	none	178.08444	178.08453	0.51
9.21	14.24	O,O-Diisobutyl thiocarbonate	C9 H18 O2 S	none	190.10220	190.10261	2.16
10.50	0.16	S,S-Diisobutyl dithiocarbonate	C9 H18 O S2	none	206.07936	206.07914	-1.07
10.64	78.64	O,S-Diisobutyl dithiocarbonate	C9 H18 O S2	none	206.07936	206.07993	2.77
11.26	0.96	O,O-Diisobutyl dithiooxalate	C10 H18 O2 S2	none	234.07427	234.07450	0.98

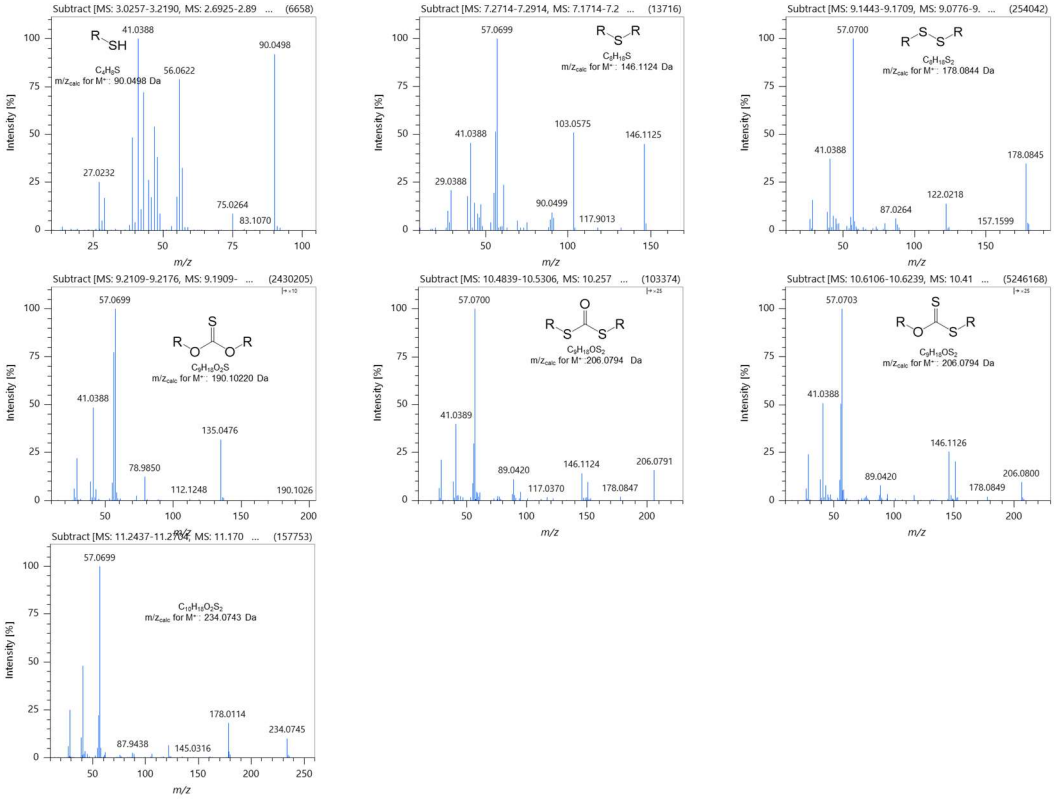

Fig. S13 Mass spectra of the decomposition products of NiXaC4b. First row: isobutane thiol, diisobutyl sulfide, diisobutyl disulfide. Second row: O,O-diisobutyl thiocarbonate, S,S-diisobutyl dithiocarbonate, O,S-diisobutyl dithiocarbonate. Third row: O,O-diisobutyl dithiooxalate.

Table S7 Pyrolysis-GC MS Data for the precursor NiXaC5, $(Ni\text{-}S\text{-}CS\text{-}OR)_2$, R = n-Pentyl). Retention times and percentages of the decomposition products with names, masses (found and calculated) and mass error

RT [min]	Area [%]	Name	Formula	Adduct/Loss	m/z calc.	m/z found	Mass error [ppm]
1.53	6.25	Carbonyl sulfide	C O S	none	59.96644	59.96653	1.50
1.76	1.15	1-Pentene	C5 H10	none	70.07770	70.07788	2.57
1.90	1.26	Carbon disulfide	C S2	none	75.94359	75.94370	1.45
4.36	2.02	1-Pentanol	C5 H12 O	-H2O	70.07770	70.07784	2.00
5.13	1.48	1-Pentane thiol	C5 H12 S	none	104.06542	104.06541	-0.10
9.71	4.12	Dipentyl sulfide	C10 H22 S	none	174.14367	174.14376	0.52
11.24	2.77	Dipentyl disulfide	C10 H22 S2	none	206.11574	206.11588	0.68
11.29	3.43	O,O-Dipentyl thiocarbonate	C11 H22 O2 S	none	218.13350	218.13406	2.57
12.50	77.53	O,S-Dipentyl dithiocarbonate	C11 H22 O S2	none	234.11066	234.11116	2.14

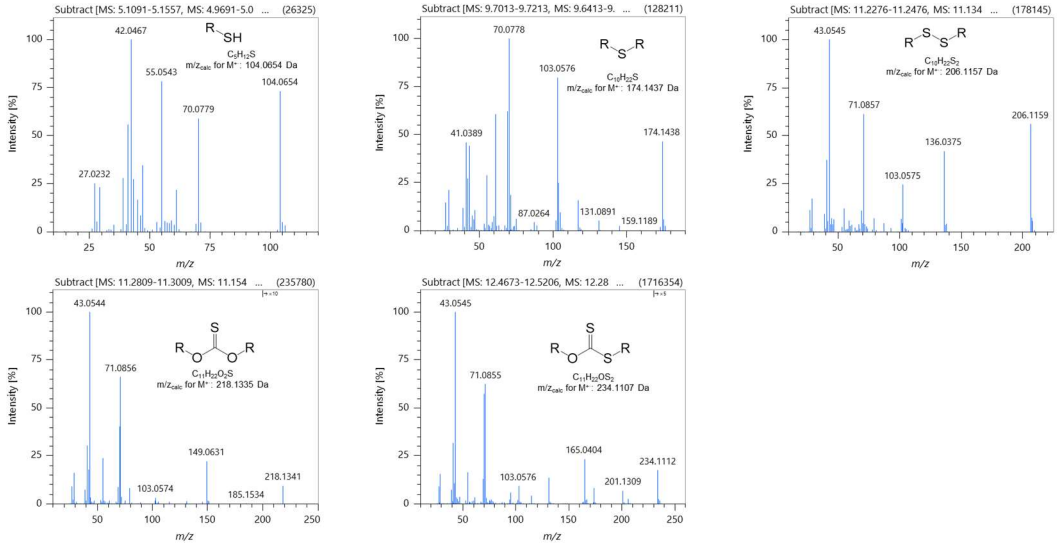

Fig. S14 Mass spectra of the decomposition products of NiXaC5. First row: pentane thiol, dipentyl sulfide, dipentyl disulfide. Second row: O,O-dipentyl thiocarbonate, O,S-dipentyl dithiocarbonate.

Table S8 Pyrolysis-GC MS Data for the precursor NiXaC5b, $(Ni\text{-}S\text{-}CS\text{-}OR)_2$, R = neo-Pentyl). Retention times and percentages of the decomposition products with names, masses (found and calculated) and mass error

RT [min]	Area [%]	Name	Formula	Adduct/Loss	m/z calc.	m/z found	Mass error [ppm]
1.56	5.60	Carbonyl sulfide	C O S	none	59.96644	59.96656	2.00
1.79	18.66	1,1-Dimethylcyclopropane	C5 H10	none	70.07770	70.07790	2.85
1.94	5.95	Carbon disulfide	C S2	none	75.94359	75.94370	1.45
2.94	2.68	Neopentanol	C5 H12 O	-CH3	73.06479	73.06498	2.60
3.89	2.32	Neopentane thiol	C5 H12 S	none	104.06542	104.06543	0.10
9.54	23.67	O,O-Dineopentyl thiocarbonate	C11 H22 O2 S	none	218.13350	218.13384	1.56
9.87	0.27	Dineopentyl disulfide	C10 H22 S2	none	206.11574	206.11585	0.53
11.04	35.72	O,S-Dineopentyl dithiocarbonate	C11 H22 O S2	none	234.11066	234.11101	1.50
11.38	1.19	S,S-Dineopentyl dithiocarbonate	C11 H22 O S2	none	234.11066	234.11084	0.77
11.54	3.95	O,O-Dineopentyl dithiooxalate	C12 H22 O2 S2	none	262.10557	262.10564	0.27

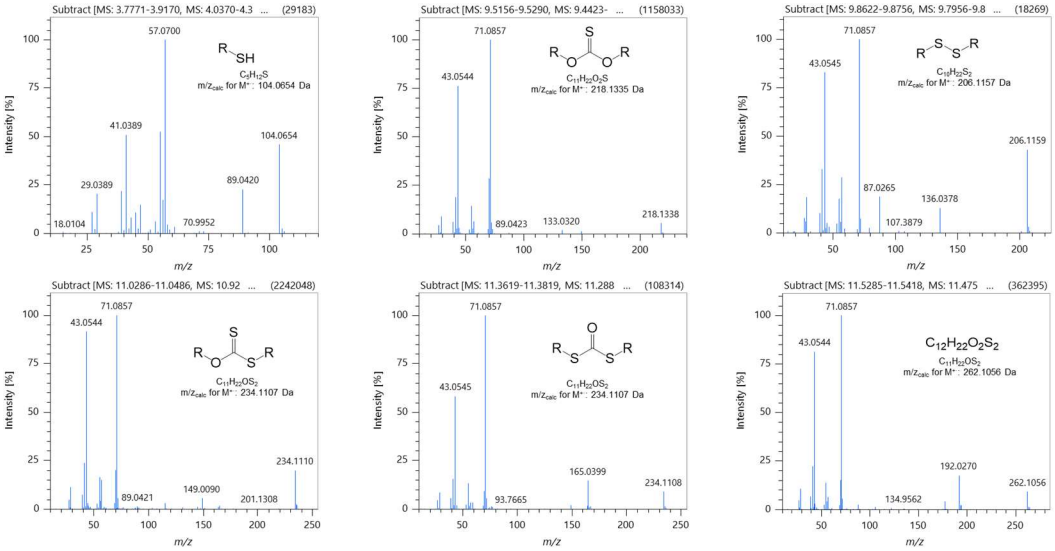

Fig. S15 Mass spectra of the decomposition products of NiXaC5b. First row: neopentane thiol, O,O-dineopentyl thiocarbonate, dineopentyl disulfide. Second row: O,S-dineopentyl dithiocarbonate, S,S-dineopentyl dithiocarbonate, O,O-dineopentyl dithiooxalate.

Table S9 Pyrolysis-GC MS Data for the precursor NiXaC6, $(Ni\text{-}S\text{-}CS\text{-}OR)_2$, R = n-Hexyl). Retention times and percentages of the decomposition products with names, masses (found and calculated) and mass error

RT [min]	Area [%]	Name	Formula	Adduct/Loss	m/z calc.	m/z found	Mass error [ppm]
1.57	2.97	Carbonyl sulfide	C O S	none	59.96644	59.96655	1.83
1.94	0.82	Carbon disulfide	C S2	none	75.94359	75.94373	1.84
2.18	0.08	1-Hexene	C6 H12	none	84.09335	84.09343	0.95
5.80	0.60	1-Hexanol	C6 H14 O	-H2O	84.09335	84.09341	0.71
6.46	0.64	1-Hexane thiol	C6 H14 S	none	118.08107	118.08113	0.51
11.10	2.10	Dihexyl sulfide	C12 H26 S	none	202.17497	202.17522	1.24
12.47	0.69	Dihexyl disulfide	C12 H26 S2	none	234.14704	234.14743	1.67
12.50	7.75	O,O-Dihexyl thiocarbonate	C13 H26 O2 S	none	246.16480	246.16536	2.27
13.67	84.35	O,S-Dihexyl dithiocarbonate	C13 H26 O S2	none	262.14196	262.14266	2.67

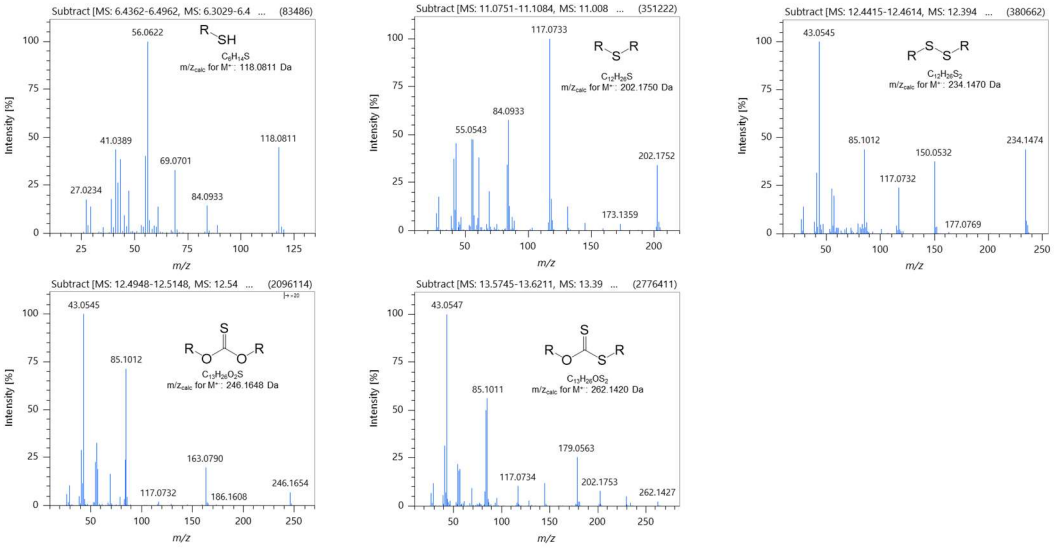

Fig. S16 Mass spectra of the decomposition products of NiXaC6. First row: hexane thiol, dihexyl sulfide, dihexyl disulfide. Second row: O,O-dihexyl thiocarbonate, O,S-dihexyl dithiocarbonate.

Table S10 Summary of the degradation product profiles of the measured NiXa precursors determined via pyrolysis-GC-MS

	Methyl	Ethyl	n-Propyl	n-Pentyl	n-Hexyl	iso-Propyl	iso-Butyl	neo-Pentyl
COS	14.82	11.35	7.38	6.25	2.97	39.36	2.45	5.60
CS2	1.78	1.81	1.46	1.26	0.82	0.35	2.66	5.95
Alkene/*Cycloalkane*			0.05	1.14	0.08		0.36	*18.66*
R-OH	0.12	0.49	0.30	2.02	0.60	0.44	0.04	2.68
R-SH	0.01	0.03	0.03	1.48	0.64	17.76	0.03	2.32
R-S-R	1.70	0.87	0.75	4.12	2.10	12.57	0.13	
R-SS-R	1.24	2.43	2.00	2.77	0.69	21.28	0.34	0.27
R-SSS-R						0.06		
R-O-CO-S-R		0.45						
R-O-CS-O-R	1.99	2.53	4.14	3.43	7.75	0.22	14.24	23.67
R-O-CS-S-R	78.05	79.86	83.54	77.52	84.34	0.89	78.64	35.72
R-S-CO-S-R	0.04					7.05	0.16	1.19
R-O-CS-CS-O-R	0.26	0.18	0.35				0.96	3.95
R-S-CS-S-R	0.01							

X-Ray diffraction

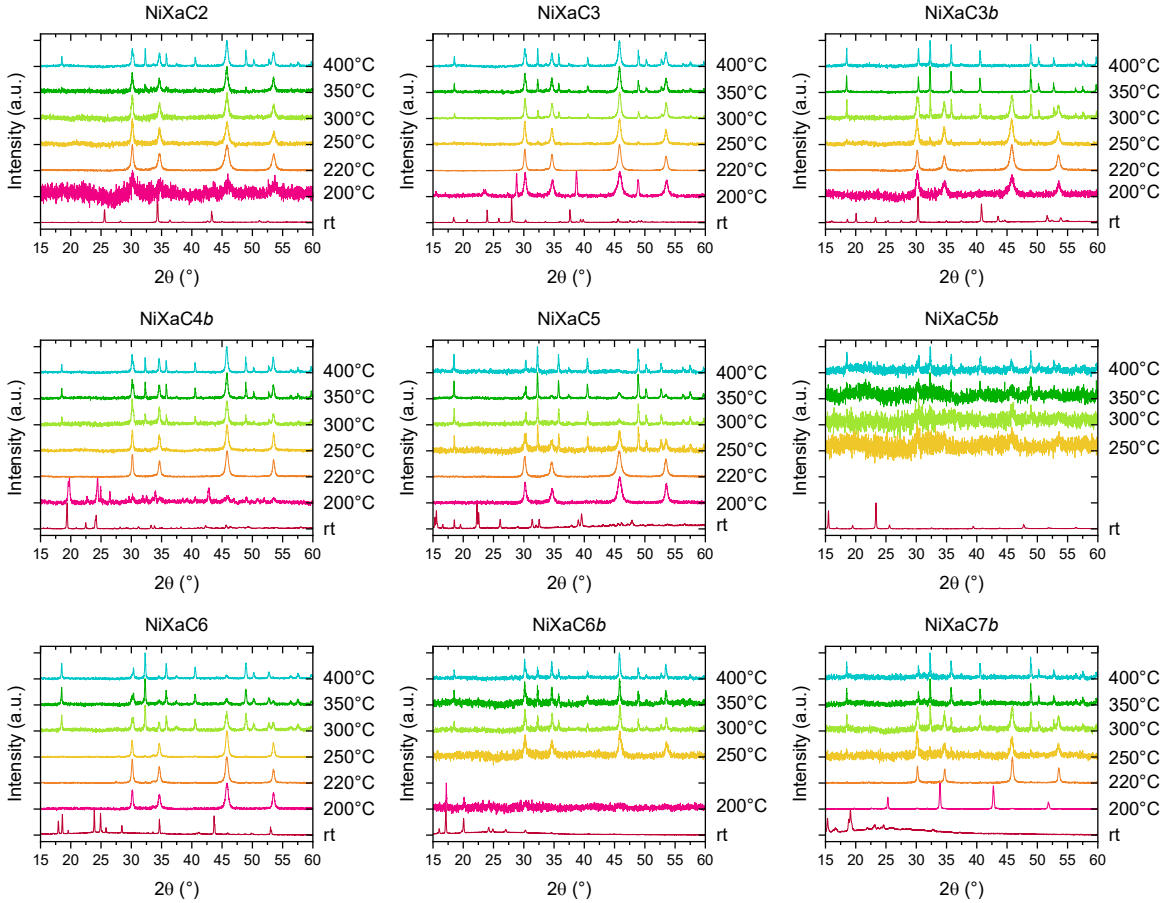

Fig. S17 XRD patterns of NiS thin films prepared from the precursors NiXaC2, NiXaC3, NiXaC3b, NiXaC4b, NiXaC5, NiXaC5b, NiXaC6, NiXaC6b, NiXaC7b by sintering at different temperatures.

Table S11 Phase composition of NiS thin films prepared from different precursors and sintered at temperatures between 200 and 400 °C. Percentages of α- and β-NiS were calculated from the intensities of the major reference reflexes (α-NiS: 102, 45.9 °2θ, β-NiS: 300, 32.2 °2θ, Fig. 6)

Compound	NiXaC2		NiXaC3		NiXaC3b		NiXaC4b		NiXaC5	
T [°C]	α [%]	β [%]	α [%]	β [%]	α [%]	β [%]	α [%]	β [%]	α [%]	β [%]
400	74	26	59	41	0	100	63	37	0	100
350	80	20	66	34	0	100	61	39	18	82
300	100	0	76	24	46	54	68	32	19	81
250	100	0	100	0	78	22	100	0	43	57
220	100	0	100	0	100	0	100	0	100	0
200	-	-	100	0	100	0	-	-	100	0
Compound	NiXaC5b		NiXaC6		NiXaC6b		NiXaC7b			
T [°C]	α [%]	β [%]	α [%]	β [%]	α [%]	β [%]	α [%]	β [%]		
400	29	71	12	88	69	31	0	100		
350	37	63	18	82	57	43	0	100		
300	-	-	43	57	65	35	47	53		
250	100	0	100	0	100	0	100	0		
220	-	-	100	0	-	-	100	0		
200	-	-	100	0	-	-	-	-		

Table S12 Primary crystallite size of the NiS thin films prepared from different precursors and sintered at temperatures between 200 and 400 °C. Primary crystallite sizes were calculated from the intensities of the major reference reflexes (α-NiS: 102, 45.9 °2θ, β-NiS: 300, 32.2 °2θ, Fig. 6)

Compound	NiXaC2		NiXaC3		NiXaC3b		NiXaC4b		NiXaC5	
T [°C]	α [nm]	β [nm]	α [nm]	β [nm]	α [nm]	β [nm]	α [nm]	β [nm]	α [nm]	β [nm]
400	18	115	18	78	-	78	23	92	-	62
350	18	52	18	78	-	92	21	78	16	62
300	16	-	17	69	16	78	19	92	17	78
250	13	-	14	-	13	92	18	-	16	78
220	11	-	14	-	11	-	14	-	11	-
200	-	-	10	-	9	-	-	-	11	-
Compound	NiXaC5b		NiXaC6		NiXaC6b		NiXaC7b			
T [°C]	α	β	α [nm]	β [nm]	α [nm]	β [nm]	α [nm]	β [nm]		
400			24	56	33	69	-	92		
350			18	52	33	69	-	92		
300			19	48	27	69	17	62		
250			18	-	16	-	16	-		
220			15	-	-	-	22	-		
200			15	-	-	-	-	-		

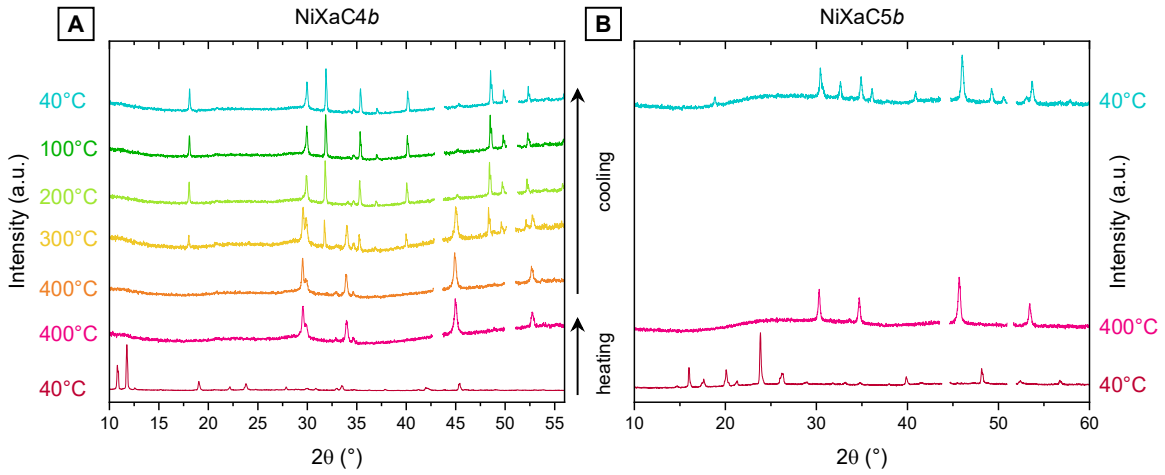

Fig. S18 XRD-heating runs. A: precursor NiXaC4b was heated up to 400 °C with a heating rate of 25 °C min^{-1}. XRD patterns were recorded at the start of the experiment, upon reaching 400 °C, after 30 mins holding time at 400 °C, and every 100 °C during cooling. The last XRD was recorded after 20 min at 40 °C. B: precursor NiXaC5b was heated up to 400 °C with a heating rate of 25 °C min^{-1}. XRD measurements were recorded at the start of the experiment, after 30 min holding time at 400 °C and after 20 min holding at 40 °C.

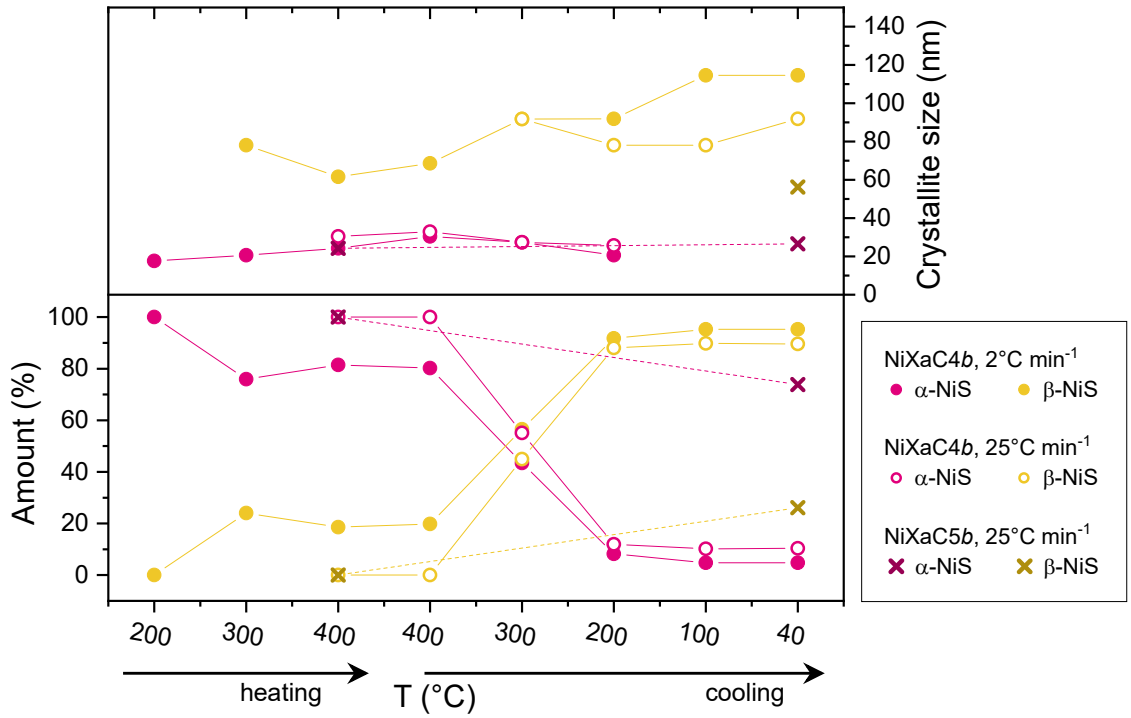

Fig. S19 XRD characterization during heating runs. Changes of phase compositions and primary crystallite sizes during the experiment for the precursors NiXaC4b and NiXaC5b with different heating rates. NiXaC4b: 2 °C min^{-1} (Fig. 7) and 25 °C min^{-1} (Fig. S18A), NiXaC5b: 25 °C min^{-1} (Fig. S18B)

Table S13 Primary crystallite sizes and percentages of α- and β-NiS calculated from the powder-XRD measurements given in Fig. 9. Powder XRD measurements were recorded of the NiS obtained from the different NiXa precursors after sintering at 400 °C, N_2. Percentage and primary crystallite sizes were calculated from the intensities of the major reference reflexes (α-NiS: 102, 45.9 °2θ, β-NiS: 300, 32.2 °2θ)

Compound	Crystallite size [nm] (α-NiS, 2θ: 45.9)	Crystallite size [nm] (β-NiS, 2θ: 48.9)	α-NiS [%]	β-NiS [%]
NiXaC1	18	-	100	0
NiXaC2	20	56	25	75
NiXaC3	19	69	9	91
NiXaC3*b*	-	92	0	100
NiXaC4*b*	21	78	17	83
NiXaC5	21	52	50	50
NiXaC5*b*	24		91	9
NiXaC6	21	45	70	30
NiXaC6*b*	27	69	26	74
NiXaC7*b*	-	134	0	100

Grazing incidence wide angle X-ray scattering

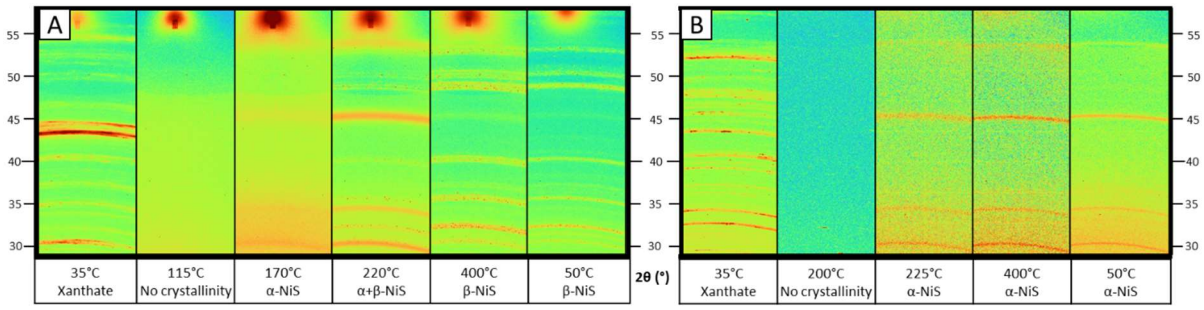

Fig. S20 2D GIWAXS images for selected temperatures from the heating runs of the precursors NiXaC3b (A) and NiXaC5b (B). The corresponding 1D integrated profiles were obtained by radial integration and are given in Fig. 8A and C and discussed in the main part. Note: The spot in A is related to the Si reflection from the wafer.

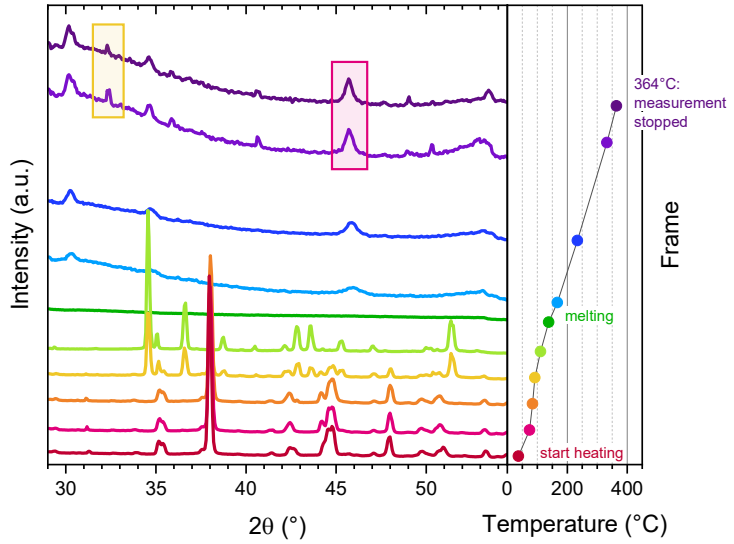

Fig. S21 Selected curves of the GIWAXS heating run for the precursor NiXaC2 up to a temperature of 364 °C (measurement aborted due to a device malfunction). Three distinct crystalline precursor phases are observable: Phase 1 up to 95 °C, Phase 2 from 84 to 95 °C, Phase 3 from 87 to 135 °C. At 138 °C the melting, marked by a loss of crystallinity, occurs, followed by the emergence of the α-NiS phase at 156 °C. The β-NiS phase starts to appear at 308 °C. Due to the measurement abort the further conversion could not be observed. Inset: last curve of the heating run (364 °C) with the major reflexes of α-NiS (45.9 °2θ, pink) and β-NiS (32.2 °2θ, yellow) highlighted. Intensity of last three lines was increased for clarity.

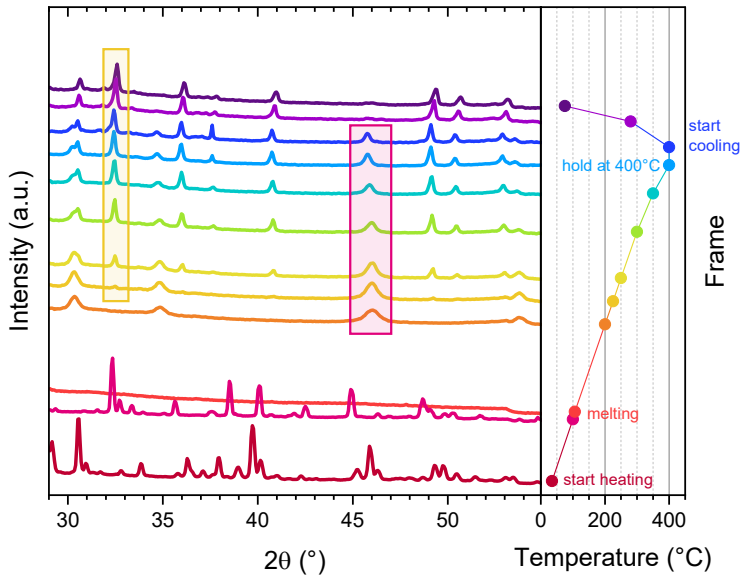

Fig. S22 Selected curves of the GIWAXS heating run for the precursor NiXaC3. Phase 1 up to 80 °C, Phase 2 from 80 to 107 °C, followed by the start of degradation at 110 °C. The α-NiS phase starts to emerge at 161 °C, the β-phase at 222 °C. Upon cooling, the amount of α-phase decreases and β-NiS with low amounts of α-NiS is obtained (6.0 % α, 94.0 % β).

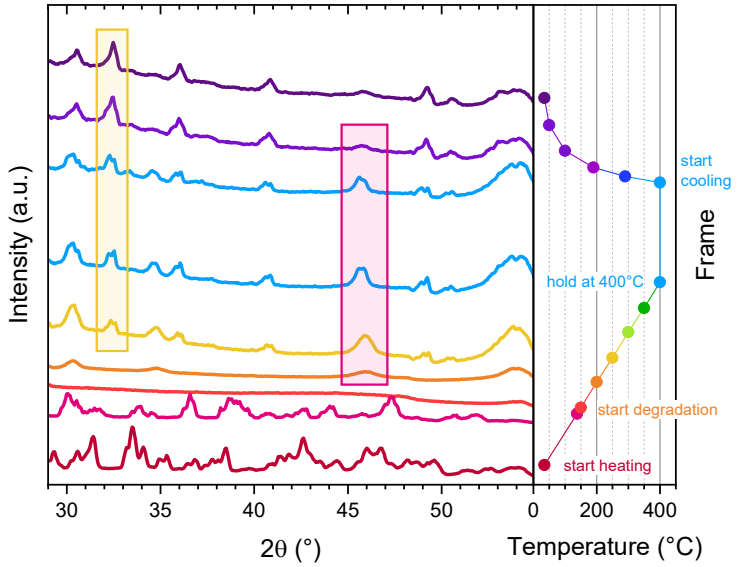

Fig. S23 Selected curves of the GIWAXS heating run for the precursor NiXaC4b. Phase 1 up to 111 °C, Phase 2 from 111 to 141 °C, followed by the start of degradation at 144 °C. The α-NiS phase starts to emerge at 188 °C, the β-phase at 231 °C. Upon cooling, the amount of α-phase decreases and a mixture of the phases with about 17.4 % α and 82.6 % β-NiS is obtained. Intensity of traces (after 250°C) was increased for clarity.

Single crystal X-ray diffraction studies

Table S14 Crystallographic data and details of measurements for the investigated nickel xanthates. R1= $\sum / |F_o| - |F_c| / \sum |F_d|$; wR2 = $[\sum_w (F_o^2 - F_2^2)^2 / \sum_w (F_o^2)^2]^{1/2}$

Compound	**NiXaC3**	**NiXaC3b**	**NiXaC4b**	**NiXaC5b**	**NiXaC6**
Reference/ CCDC no.	**Juncal et al***	**2430036**	**2430037**	**2430038**	**2430039**
Formula	$C_8H_{14}NiO_2S_4$	$C_8H_{14}NiO_2S_4$	$C_{10}H_{18}NiO_2S_4$	$C_{12}H_{22}NiO_2S_4$	$C_{14}H_{26}NiO_2S_4$
Fw (g mol^{-1})	329.14	329.14	357.19	385.24	413.30
a (Å)	7.4677(1)	8.6758(2)	6.0035(1)	6.2156(3)	6.7876(2)
b (Å)	9.4726(1)	6.0221(1)	8.0661(1)	6.3279(3)	7.5569(3)
c (Å)	9.8244(1)	13.1843(3)	8.7554(1)	11.3967(5)	10.4461(4)
α (°)	73.457(1)	90	110.160(1)	80.452(4)	101.898(3)
β (°)	86.868(1)	93.795(2)	99.113(1)	89.570(3)	98.291(3)
γ (°)	74.876(1)	90	104.281(1)	86.522(4)	111.480(3)
V (Å^3)	642.98(1)	687.32(3)	371.64(1)	441.23(4)	473.47(3)
Z	2	2	1	1	1
Crystal size (mm)	0.16 × 0.12 × 0.11	0.17 × 0.1 × 0.05	0.19 × 0.10 × 0.06	0.19 × 0.14 × 0.01	0.19 × 0.09 × 0.05
Crystal habit	Block, orange	Block, orange	Block, orange	Plate, yellow	Plate, light orange
Crystal system	Triclinic	Monoclinic	Triclinic	Triclinic	Triclinic
Space group	*P*-1	$P2_1/c$	*P*-1	*P*-1	*P*-1
d_{calc} (Mg m^{-3})	1.700	1.590	1.596	1.450	1.449
μ (mm^{-1})	8.08	7.56	7.04	5.97	5.60
Radiation type	Cu K_α	Cu K_α	Cu K_α	Cu K_α	Cu K_α
Wavelength (Å)	1.54056	1.54056	1.54056	1.54056	1.54056
T (K)	100(2)	100(2)	100(2)	100(2)	100(2)
ϑ range (°)	4.7–78.5	3.3–78.9	5.6–77.2	3.9–77.5	4.4–77.0
F(000)	340	340	186	202	218
T_{min}, T_{max}	0.601, 0.878	0.446, 0.869	0.413, 1.000	0.450, 1.000	0.040, 0.361
R_{int}	0.022	0.029	0.010	0.050	0.033
No. of measured, independent, and observed [$I > 2\sigma(I)$] reflections	27199, 2715, 2670	28194, 1467, 1460	7771, 1566, 1561	16270, 1756, 1687	8834, 1855, 1750
independent reflections	2715	1467	1566	1756	1855
No. of parameters, restraints	193, 0	98, 0	116, 0	122, 0	98, 0
Δρmax, Δρmin (e Å^{-3})	0.33, -0.24	0.69, -0.37	0.35, -0.20	1.95, -0.73	2.43, -0.71
GooF	1.10	1.11	1.07	1.13	1.087
R1, wR2 (all data)	R1 = 0.0168 wR2 = 0.0458	R1 = 0.0257 wR2 = 0.0692	R1 = 0.0169 wR2 = 0.0446	R1 = 0.0722 wR2 = 0.2048	R1 = 0.0729 wR2 = 0.1762
R1, wR2 (>2σ)	R1 = 0.0166 wR2 = 0.0456	R1 = 0.0256 wR2 = 0.0692	R1 = 0.0168 wR2 = 0.0446	R1 = 0.0704 wR2 = 0.2025	R1 = 0.0718 wR2 = 0.1741

* L. C. Juncal, E. G. Ferrer, P. A. M. Williams, R. Boese, C. G. Pozzi, C. O. Della Védova and R. M. Romano, *Chemical Physics Letters*, 2022, **794**, 139487.

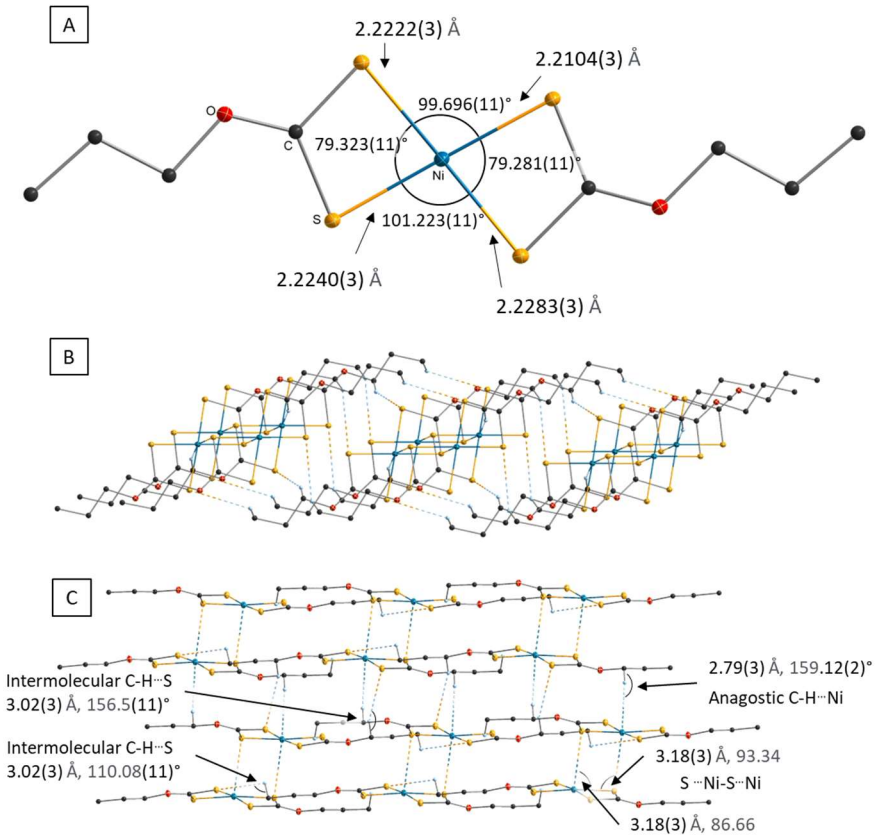

Fig. S24 (A) Crystal structure diagram for NiXaC3 with M-S bond lengths and angles. The views along the crystallographic axes a and c are given in (B) and (C), respectively. The compound NiXaC3 crystallizes as 3D network propagated by C−H···S hydrogen bonds and C−H···Ni anagostic interactions. All non-carbon atoms shown as 30% shaded ellipsoids. Hydrogen atoms not involved in intermolecular interactions omitted for clarity. Ni-S bonds and angles are not symmetric and slightly distorted. Intermolecular C-H···S interactions occur both along the plane (formed by the distorted square planar Ni-S, see **Fig. S25**) and between the layers. The interaction of each nickel center with a neighboring H (anagostic) and an opposite S (intermolecular) forms a H···Ni···S angle of 168.99 °.

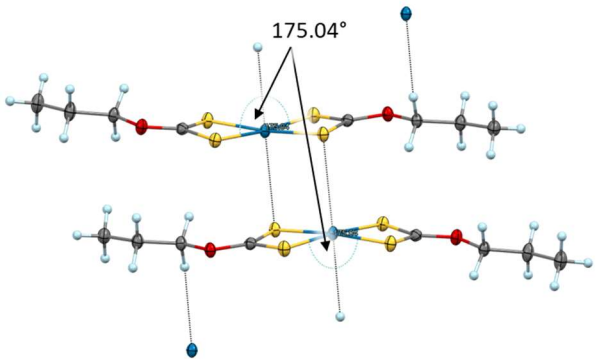

Fig. S25 Z-distortion of the nickel atom in the center of the plane formed by the 4 sulfur atoms. Nickel atoms from neighboring planes are displaced from the plane in opposing directions.

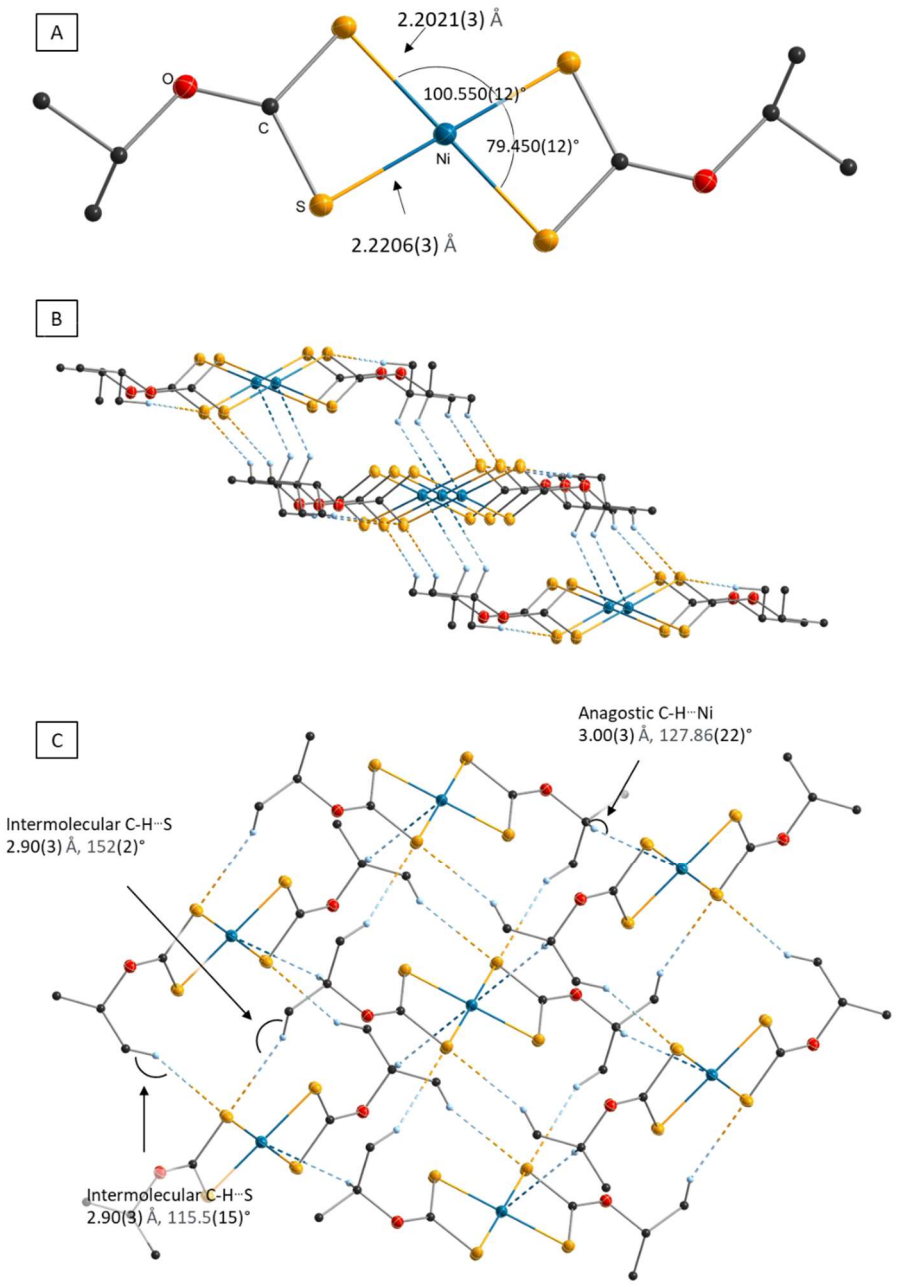

Fig. S26 (A) Crystal structure diagram for NiXaC3b , with the view along c (B) and b (C). The compound NiXaC3b crystallizes as 3D network propagated by C−H···S hydrogen bonds and C−H···Ni anagostic interactions. All non-carbon atoms shown as 30% shaded ellipsoids. Hydrogen atoms not involved in intermolecular interactions omitted for clarity. Ni-S bonds and angles are symmetric. Each Ni center is involved in two anagostic C-H···Ni interactions trans to each other, forming a H···Ni···H angle of 180 °. Intermolecular C-H···S interactions between 3 molecules form an 80.4 ° angle between H···S···H.

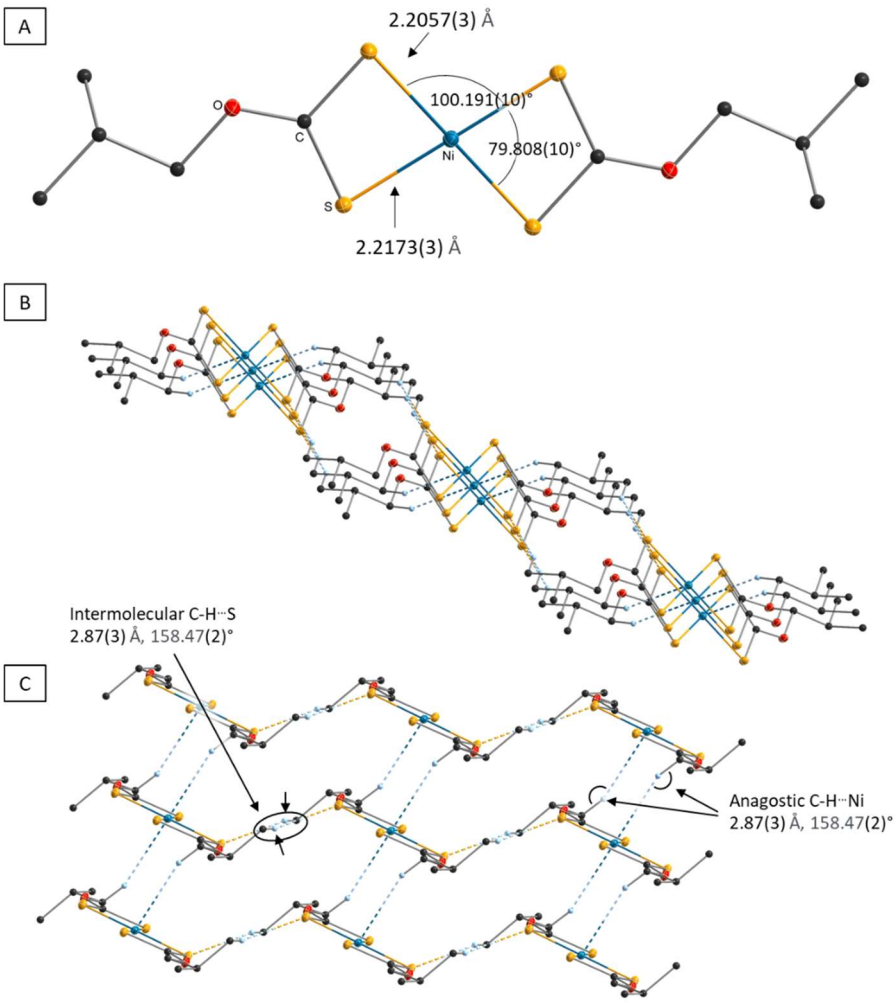

Fig. S27 (A) Crystal structure diagram for NiXaC4b, with the view along a (B) and c (C). The compound NiXaC4b crystallizes as 3D network propagated by C–H···S hydrogen bonds and C–H···Ni anagostic interactions. All non-carbon atoms shown as 30% shaded ellipsoids. Hydrogen atoms not involved in intermolecular interactions omitted for clarity. Ni-S bonds and angles are symmetric (A). Each Ni center is involved in two anagostic C-H···Ni interactions trans to each other forming a H···Ni···H angle of 180 °.

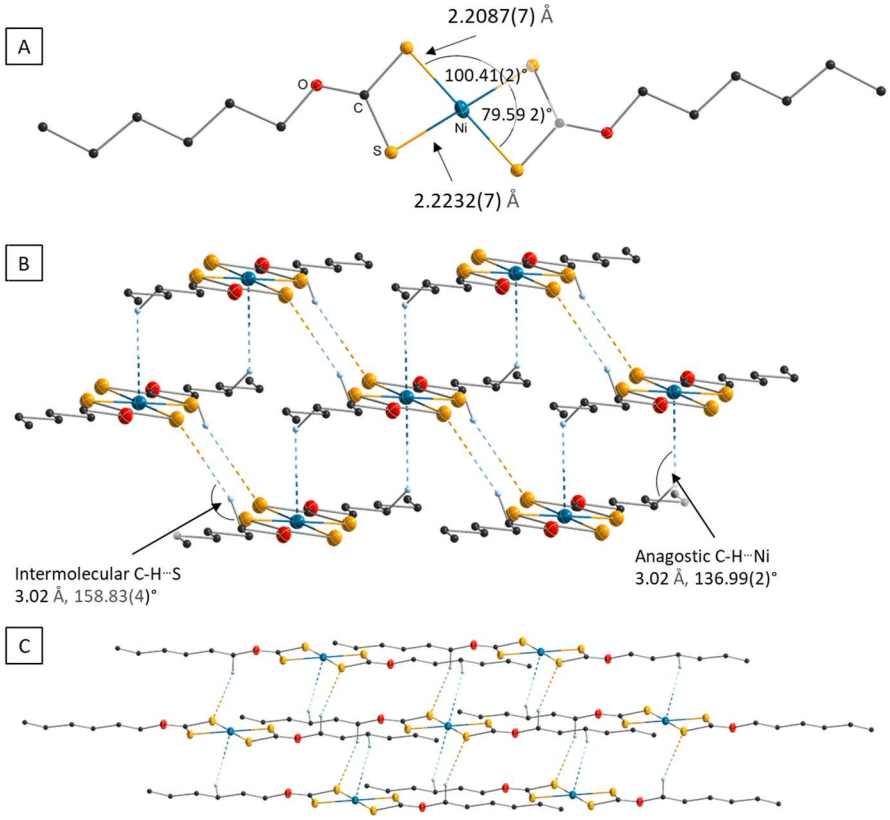

Fig. S28 Crystal structure diagram for NiXaC6, with the view along b (B) and c (C). The compound NiXaC6 crystallizes as 3D network propagated by C–H···S hydrogen bonds and C–H···Ni anagostic interactions. All non-carbon atoms shown as 30% shaded ellipsoids. Hydrogen atoms not involved in intermolecular interactions omitted for clarity. Each Ni center is involved in two anagostic C-H···Ni interactions trans to each other forming a H···Ni···H angle of 180 °.